COLLISIONAL GRANULAR FLOWS WITH AND WITHOUT GAS INTERACTIONS IN MICROGRAVITY

Michel Y. Louge and Haitao Xu
Sibley School of Mechanical and Aerospace Engineering
Cornell University
Ithaca, NY 14850 USA
MYL3@cornell.edu

Abstract   We illustrate the convenience of a long-lasting microgravity environment to study flows of granular materials with and without gas interaction. We consider collisional granular flows of nearly elastic identical spheres in an axisymmetric Couette channel featuring two cylindrical moving bumpy boundaries and two flat walls. We review governing equations for these flows, illustrate their solutions and compare them with numerical simulations.

Keywords: Gas-solid interaction, microgravity, granular flows

Introduction

Flows of gases loaded with granular materials occur in nature and in industrial processes. On Earth, applications are found in the chemical, mining and pharmaceutical industries. The long-term human or robotic exploration of the Moon and Mars requires the development of "In-Situ Resource Utilization" for propellant production, habitat, infrastructure, and extraction of water and breathable gas. These new technologies all require a deeper understanding of interactions among grains and between grains and gases. On the particle scale, viscous hydrodynamic interactions and grain collisions are a crucial attribute of the physics.

In such processes, collisions induce agitation among grains that is quantified by the "granular temperature" $T \equiv (1/3)\overline{u'_i u'_i}$, in which u'_i is the fluctuation velocity along the direction i. Defined by analogy with the translational temperature of a hard-sphere gas, the granular temperature is responsible for the transport of momentum among grains

interacting through brief collisions [1]. It plays a central role in suspensions of gases and agitated solids.

In the absence of gravity, sheared suspensions of spherical grains in a gas are characterized by three dimensionless numbers. The Stokes number $St \equiv \tau_v \Gamma$ measures the relative importance of grain inertia and viscous forces acting on a sphere of viscous relaxation time $\tau_v = \rho_s d^2 / 18 \mu_g$, where ρ_s is the material density of the sphere, d is its diameter, μ_g is the gas viscosity, and Γ is the applied shear rate. For its part, the Reynolds number compares fluid inertia and viscous forces. It may be based on shear rate, $Re \equiv \rho_g \Gamma d^2 / \mu_g$, where ρ_g is the gas density; or on granular temperature, $Re_T \equiv \rho_g \sqrt{T} d / \mu_g$; or on the difference between the mean gas velocity u_g and its counterpart u_s for the solids in the flow direction x, $Re_{slip} \equiv \rho_g |u_g - u_s| d / \mu_g$. If the suspensions involve such relative velocity, the corresponding mean gas pressure gradient dP_g/dx is made dimensionless with $R_\tau \equiv (-dP_g/dx)/\rho_s \Gamma^2 d$.

In this work, we plan to exploit long-lasting microgravity to isolate the effects of hydrodynamic forces from those of gravitational accelerations in generic flows of granular materials with and without significant gas interaction. This paper briefly outlines this effort.

We begin with an overview of the objectives of the project. We then sketch the theories that we used to design the experiments. Finally, we illustrate the nascent promise of Lattice-Boltzmann (LB) simulations by comparing their results with theory for particles colliding in a gas within a bounded flow geometry.

1.   Objectives

NASA is designing an axisymmetric Couette shear cell to accommodate three experiments in granular segregation and gas-solid interactions (Fig. 1). In the first, we will observe the segregation of a binary mixture of granular materials that collide with each other and with the moving boundaries of the cell at a Stokes number large enough that the gas plays no role. In the absence of gravity, the only segregation mechanism is driven by gradients of the granular temperature [2]. We discussed the corresponding theories, simulations and experiments at ICTAM 2000 [3, 4], and will not repeat these here for conciseness.

The second series of tests involves "Viscous/Dissipation Experiments". Here, the motion of the boundaries is progressively slowed, and thus the Stokes number is reduced, until the dissipation of granular temperature by viscous forces in the gas dominates its counterpart due to inelastic collisions [5]. In these experiments, the mean relative velocity between
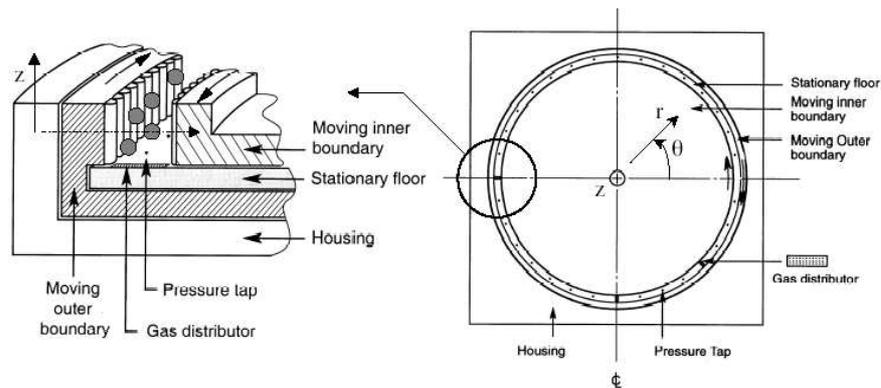
Collisional Granular Flows with and without Gas Interactions...   3

Figure 1. Sketch of the axisymmetric Couette cell. It is described by cylindrical coordinates centered on the rotation axis of the moving cylindrical rough boundaries half-way between the planes of the flat side walls. When $R_\tau \neq 0$, gas is introduced at $\theta = 0$ and withdrawn at $\theta = \pi$. Left: detail near $\theta = \pi$ shown without the top flat cover.

solids and gases is negligible, $R_\tau = 0$, and we typically keep Re_T low as well.

In the third kind of tests, called "Viscous Drag Experiments", we introduce and withdraw gas through distributors at opposite ends along the rectangular channel of the cell, thus creating a mean relative velocity and, consequently, a mean drag between solids and gas. Pressure taps are located at regular intervals on the rear flat wall to monitor the corresponding evolution of the static gas pressure along the channel. Further gas is injected through a distributor located at $\theta = 7\pi/4$ to create an "isokinetic" region with $P_g(\theta = 7\pi/4) = P_g(\theta = 0)$. Because $u_s \approx u_g$ in that region, it is possible to infer the gas volume flow rate there from a measurement of the mean granular velocity and volume fraction [6, 7].

The microgravity shear cell will thus create suspensions in a range of laminar, steady, fully developed conditions where viscous forces dominate the gas flow and inertial forces proportional to the gas density are nearly eliminated. Unlike terrestrial flows, where the gas velocity must be set to a value large enough to support the weight of particles, microgravity of sufficient duration and quality [7] will permit us to control the agitation of the particles and the gas flow independently by adjusting the pressure gradient along the flow and the relative motion of the boundaries.

An important outcome of these experiments will be to validate numerical simulations of the flow. In the Viscous Dissipation and Viscous Drag experiments we will compare profiles of granular velocity, tem-

perature and species volume fraction that are observed using computer vision techniques [8] against those predicted by LB simulations like those of Ladd [9]. We anticipate that these simulations will soon be capable of handling our entire microgravity shear cell, and thus allow direct comparisons with profiles of granular velocity and temperature.

Once such simulations are validated in these experiments, they can inform the development of constitutive relations, and extrapolate to situations where the grains are neither spherical nor monodisperse.

2.   Theory

We sketch here the outlines of a theory that we have used to design the experiments. We consider steady collisional flows of nearly elastic, nearly frictionless grains featuring a single constituent of identical spheres in a gas. Because the "Viscous Dissipation" experiments are conducted in an axisymmetric channel, their flows are everywhere fully-developed along the polar angle θ shown in Fig. 1. We also extend the analysis to regions of the "Viscous Drag" experiments where the flow has reached a nearly fully-developed state with $dP_g/d\theta = $ constant. By integrating the flow in the channel cross-section, Xu [7] and Xu et al. [10] calculated the flow development and predicted where such fully-developed regions can be observed.

We begin by discussing the role of centripetal accelerations in the simpler case of a monodisperse flow of spheres without interstitial gas or gravity. When the mean velocity has no components in the radial and axial direction, then the granular momentum balance in the outward radial direction r reduces to

$$\frac{dP_s}{dr} = \rho_s \nu \frac{u_s^2}{r}, \tag{1}$$

where ν is the solid volume fraction and $u_s = u_s(r, z)$ is the mean velocity in azimuthal direction.

The importance of centripetal accelerations can be estimated by comparing variations of the granular pressure along the radial direction with its magnitude

$$P_s = \rho_s \nu (1 + 4G)T. \tag{2}$$

Combining Eqs. (1) and (2) we find that the relative change in granular pressure ΔP_s from the inner to the outer wall scales as

$$\frac{\Delta P_s}{\overline{P_s}} \sim \left(\frac{\Delta R}{\overline{R}} \right) \left(\frac{\overline{u_s}^2}{(1 + 4G)\overline{\overline{T}}} \right), \tag{3}$$

Collisional Granular Flows with and without Gas Interactions...   5

where the overbar denotes the typical magnitude of a quantity in the channel, ΔR is the distance between the two cylindrical moving boundaries, and $\overline{R}$ is the average radius of the channel. Because in the absence of gravity or gas $\overline{u_s}^2$ and $\overline{T}$ both scale as the square of the boundary velocity, the second parenthesis of Eq. (3) is independent of the rotation rate of the cell boundaries. Thus, the effects of centripetal acceleration are only minimized by operating a cell with a distance $\Delta R \ll \overline{R}$. Our calculations indicate that, for typical flows, $\Delta P_s/P_s < 10\%$ for $\Delta R/\overline{R} < 1/15$.

A convenient way to circumvent the complexity presented by variations of flow variables in two dimensions r and z is to integrate the balance equations in the direction perpendicular to the flat side walls. Because the latter are nearly elastic and frictionless, the flow variables hardly vary in the depth z from one side wall to the other. Then, we can integrate the momentum and energy balance equations in that direction by assuming that u_g, u_s, T and ν are functions of r only [4]. For simplicity, we assume here that both flat walls are identical. (Xu relaxed that assumption for a rectilinear flow [7]). To facilitate integration of the balance of fluctuation energy, we follow Jenkins and Arnarson [11] in assuming that shear stresses on surfaces perpendicular to z vary linearly between the side walls separated by a distance W, $\tau_{\theta z} = \tau_{\theta z_0} 2z/W$.

We now consider the case where the viscous gas plays a significant role in the balances of momentum and fluctuation energy. Upon integration along z, the solid momentum balance in the azimuthal flow direction becomes

$$\frac{1}{r^2}\frac{d}{dr}\left[\eta_s r^3 \frac{d}{dr}\left(\frac{u_s}{r}\right) + \nu R_\mu \mu_g r^3 \frac{d}{dr}\left(\frac{u_g}{r}\right)\right] + \frac{2}{W}\left(\tau_{\theta z_0}^s + \tau_{\theta z_0}^{gs}\right)$$

$$+\beta(u_g - u_s) - \nu\frac{1}{r}\frac{dP_g}{d\theta} = 0, \quad (4)$$

where $\eta_s = (8J/5\sqrt{\pi})\rho_s \nu G T^{1/2} d$ is the granular viscosity [1] with

$$J \equiv 1 + (\pi/12)(1 + 5/8G)^2, \quad G = \nu(2-\nu)/[2(1-\nu)^3]$$

and $\tau_{\theta z_0}^s$ is the granular shear stress function of r at $z = W/2$. The second term in straight brackets represent the stress exerted by grains on each other through the viscous gas [12]. At the flat side walls, it is $\tau_{\theta z_0}^{gs}(r)$. Inspired by the expression of Happel and Brenner [13] for the effective viscosity $\mu_g R_\mu$ of a mixture of spheres suspended in a viscous fluid, we assume that the shear stress exerted among solids through the gas is proportional to the solid volume fraction and the mixture shear

stress with $R_\mu \approx \exp(4.58\nu)$. Thus, for example, it is

$$\tau_{\theta z_0}^{gs}(r) = \nu R_\mu \mu_g (\partial u_g / \partial z)_{z=W/2} \qquad (5)$$

at the front side wall.

The remainder of the mixture shear stress belongs to the gas phase. In this view, neglecting the inertia of the gas, the steady, fully-developed gas momentum balance in the radial direction is $(dP_g / dr) = 0$, where P_g is a function of θ only. Along the flow, it is

$$\frac{1}{r^2} \frac{d}{dr} \left[(1-\nu) R_\mu \mu_g r^3 \frac{d}{dr} \left(\frac{u_g}{r} \right) \right] + \frac{2}{W} \tau_{\theta z_0}^g$$

$$- \beta(u_g - u_s) - (1-\nu) \frac{1}{r} \frac{dP_g}{d\theta} = 0, \qquad (6)$$

where

$$\tau_{\theta z_0}^g(r) = (1-\nu) R_\mu \mu_g (\partial u_g / \partial z)_{z=W/2} \qquad (7)$$

at the front side wall. The drag between gas and solids is captured by the coefficient $\beta = 18 \mu_g \nu (1-\nu)^2 R_{drag}(\nu)/d^2$. Koch and Sangani [22] determined R_{drag} from numerical simulations in the range $0 < \nu \leqslant 0.4$, and adopted Carman's expression for $\nu > 0.4$ [14]. Van der Hoef et al. fitted the results of their LB simulations with $R_{drag} = [10\nu/(1-\nu)^3] + (1-\nu)(1+1.5\sqrt{\nu})$ and obtained similar numerical results [15].

In the axisymmetric geometry, the balance of granular fluctuation energy has the form

$$\frac{1}{r} \frac{d}{dr} \left(r\kappa \frac{dT}{dr} \right) + \frac{2q_{z_0}}{W} + \eta_s \left[r \frac{d}{dr} \left(\frac{u_s}{r} \right) \right]^2 + \frac{\tau_{\theta z_0}^s{}^2}{3\eta_s}$$

$$+ \nu \mu_g R_\mu \left[r \frac{d}{dr} \left(\frac{u_g}{r} \right) \right] \left[r \frac{d}{dr} \left(\frac{u_s}{r} \right) \right] + \frac{\tau_{\theta z_0}^s \tau_{\theta z_0}^{gs}}{3\eta_s} - \gamma_s - \gamma_g + \gamma_{gs} = 0, \quad (8)$$

where $\kappa = (4M/\sqrt{\pi}) \rho_s \nu G d\sqrt{T}$ is the granular conductivity of fluctuation energy with $M \equiv 1 + (9\pi/32)(1 + 5/12G)^2$, and $q_{z_0}(r)$ is the flux of fluctuation energy into the flow through either the front or the rear flat side wall.

In Eq. (8), the last three terms represent volumetric rates of dissipation and production of fluctuation energy. The collisional dissipation rate for nearly elastic, frictionless spheres is

$$\gamma_s = (12/\sqrt{\pi})(1-e^2) \rho_s \nu T^{3/2} G/d, \qquad (9)$$

where e is Newton's kinematic coefficient of normal restitution. For slightly frictional spheres, Jenkins and Zhang calculated an effective

restitution coefficient that takes into account the energy lost by tangential impulses in an impact [16]. Goldhirsch discusses the challenges involved in establishing a rigorous theoretical framework for handling spheres with arbitrary elasticity and friction [17].

Using theoretical calculations for dilute simple shear flows, and numerical simulations at greater solid volume fractions, Sangani, Koch and others calculated the dissipation due to the viscous gas at low Re_T [18, 5],

$$\gamma_g = 54\mu_g T\nu R_{diss}(\nu, \epsilon_m)/d^2, \tag{10}$$

where

$$R_{diss} \simeq 1 + \frac{3\nu^{1/2}}{\sqrt{2}} + \frac{135\nu \ln \nu}{64} + 7.422\nu + G\ln(1/\epsilon_m). \tag{11}$$

Sundararajakumar and Koch calculated $\epsilon_m \simeq 9.76\lambda_g/d$, where λ_g is the molecular mean free path of the gas [19]. Recently, Wylie et al. [20] and Verberg and Koch [21] extended these results to higher Re_T.

Finally, mean velocity differences between gas and solids produce fluctuation energy. Koch and Sangani [22] calculated

$$\gamma_{gs} = \frac{162\mu_g^2\nu(1-\nu)^2}{\rho_s d^3 \sqrt{T}}|u_g - u_s|^2 S^*(\nu), \tag{12}$$

where

$$S^* = \frac{\nu R_{drag}^2}{2\sqrt{\pi}G(1 + 3.5\nu^{1/2} + 5.9\nu)}. \tag{13}$$

Our experience is that γ_{gs} has a relatively small effect on most flows of interest.

To close Eqs. (4) and (8), we evaluate $\tau_{\theta z_0}^s(r)$ and q_{z_0} using boundary conditions for flat, frictional planes [23] that provide $\tau_{\theta z_0}^s/P_s$ and $q_{z_0}/P_s\sqrt{T}$ in terms of impact parameters, such as restitution and friction, and in terms of the dimensionless relative velocity at the contact point, which we assume equal to $u_s/\sqrt{T}$ [4].

A separate calculation is needed to find the stresses $\tau_{\theta z_0}^{gs}(r)$ and $\tau_{\theta z_0}^g(r)$ appearing in Eqs. (4) and (6). To that end, as Eqs. (5)–(7) suggest, we must estimate the gas velocity gradient at the flat walls. We do so by considering the idealized case of a two-dimensional simple shear flow of gas and particles confined between two infinite flat plates parallel to the flow and perpendicular to the vorticity axis. We ignore the effect of the plates on particles and assume that the particle phase is homogeneous with a mean velocity profile $u_s = \Gamma y$. Applying the "no-slip" gas boundary condition at the flat plates to the two-dimensional gas momentum

balance

$$\frac{\partial}{\partial y}\left((1-\nu)R_\mu\mu_g\frac{\partial u_g}{\partial y}\right) + \frac{\partial}{\partial z}\left((1-\nu)R_\mu\mu_g\frac{\partial u_g}{\partial z}\right)$$
$$-\beta(u_g - u_s) - (1-\nu)\frac{dP_g}{dx} = 0, \qquad (14)$$

we find the analytical solution

$$u_g = \left(\Gamma y - \frac{(1-\nu)}{\beta}\frac{dP_g}{dx}\right)\left[1 - \frac{\cosh(kz/W)}{\cosh(k/2)}\right], \qquad (15)$$

where

$$k \equiv \frac{W}{d}\sqrt{18\nu(1-\nu)\frac{R_{drag}}{R_\mu}}. \qquad (16)$$

Because $W/d \gg 1$ and $k \gg 1$ in typical cases of interest, the average gas velocity in the y-direction is almost equal to its maximum value in Eq. (15), and the velocity gradient at the wall is, to a good approximation,

$$\left.\frac{\partial u_g}{\partial z}\right|_{z=W/2} \approx -\frac{k}{W}u_g, \qquad (17)$$

where u_g now indicates the gas velocity averaged from one side wall to the other. In turn, this yields $\tau_{\theta z_0}^{gs}(r)$ and $\tau_{\theta z_0}^g(r)$ from Eqs. (5) and (7).

Once closed in this way, the integral Eqs. (1), (4) and (8) are solved subject to boundary conditions at the moving bumpy boundaries. In our experiments, these walls are made of cylinders with axis parallel to the rotation axis. Xu [7] and Xu et al. [4] report the corresponding stress ratio $\tau_{r\theta}^s/P_s$ and dimensionless flux in the r-direction $q_r/P_s\sqrt{T}$ at the walls. Boundary conditions for the derivatives du_s/dr and dT/dr are then calculated by matching the prescriptions of $\tau_{r\theta}^s$ and q_r to their respective constitutive relations in the interior at the radial location of the center of a sphere in contact with the crest of a wall bump.

A difficulty arising from the simultaneous use of continuum equations for gas and solids is that the locations where their respective boundary conditions are applied do not coincide. In the gas, the usual "no-slip" condition arises at the wall, while boundary conditions of the kinetic theory concern particles with center located a sphere radius away from the crest of wall bumps. Fortunately, because our flows have relatively large volume fraction and Stokes number, the mean and fluctuation velocity of the solids and the solid stresses are not sensitive to the precise position where u_g matches the boundary velocity. Under these conditions, the mean gas velocity quickly rises to a value that is consistent with the imposed gas pressure gradient and the drag force

within a short distance from the wall. Thus, for simplicity, we ignore this difficulty and solve the gas and solid phases in the same domain $r \in [R_i + (d_i + d)/2, R_o - (d_o + d)/2]$, where R_i and R_o are the radial positions of the center of boundary bumps on the inner and outer moving boundaries, respectively, and d_i and d_o are the bump diameters on these respective boundaries. However, because the spheres can contribute mass to a volume bounded by the bump crests and the flat walls, we define the overall solid volume fraction $\bar{\nu}$ in the apparatus as the total volume of all spheres divided by the volume of a domain within $r \in [R_i + d_i/2, R_o - d_o/2]$, $\theta \in [0, 2\pi]$ and $z \in [-W/2, +W/2]$.

3.   Results

It is common for granular theories to consider unbounded simple shear flows. However, the latter only exist in numerical simulations that are periodic in the flow and vorticity directions and that apply the "Lees-Edwards" wrapping artifact across the sheared boundaries of the simulation domain [24]. In particular, the Lees-Edwards condition ensures that there is no velocity jump and no flux of fluctuation energy across those boundaries. Unfortunately, because it is impossible to engineer physical walls that have no dissipation and no slip, real experiments cannot exhibit profiles of flow variables that are consistent with simple shear. The principal contribution of the theory outlined in the previous section is to predict profiles that a practical experiment design can generate.

Comparisons with experiments must wait for the availability of a long-term microgravity platform. In the meantime, we illustrate how the theory can be used by comparing its predictions with the recent periodic LB simulations of Verberg and Koch [21], who considered rectilinear sheared flows of elastic frictionless spheres in a viscous gas between two infinite parallel boundaries with spherical bumps arranged on a nearly hexagonal planar lattice. Xu et al. calculated the corresponding boundary conditions and solved the more straightforward governing equations for this one-dimensional rectilinear geometry. Figure 2 is a snapshot of the simulations. Figure 3 shows lateral profiles of granular temperature at decreasing values of the Stokes number $St \equiv [\rho_s d^2 U]/[18\mu_g H]$, where U is the relative velocity of the two moving boundaries and H is the distance between bump crests. Here, $\bar{\nu}$ is the volume of all particles divided by H and by the other two periodic dimensions of the simulations. As Fig. 3 indicates, the theory has merit down to $St \sim 15$. Below this value, the velocity distribution function of the spheres is affected by the gas in a manner that the theory has yet to predict well.
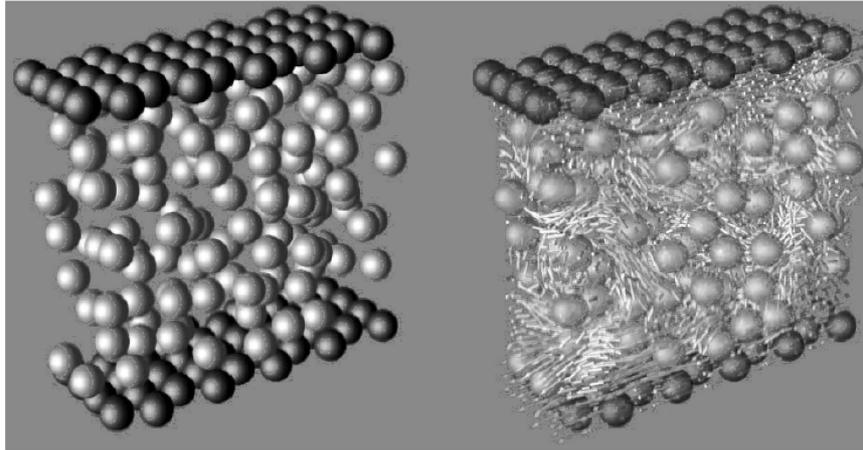
Figure 2.   Snapshot of the simulations of Verberg and Koch [21, 12] for the conditions $\bar{\nu} = 0.19$, $St = 30$, $Re = 0.8$, $H/d = 8.22$, $\rho_s/\rho_g = 675$, and $R_\tau = 0$. Left: only particles are shown; right: same realization with gas velocity vectors and particles.
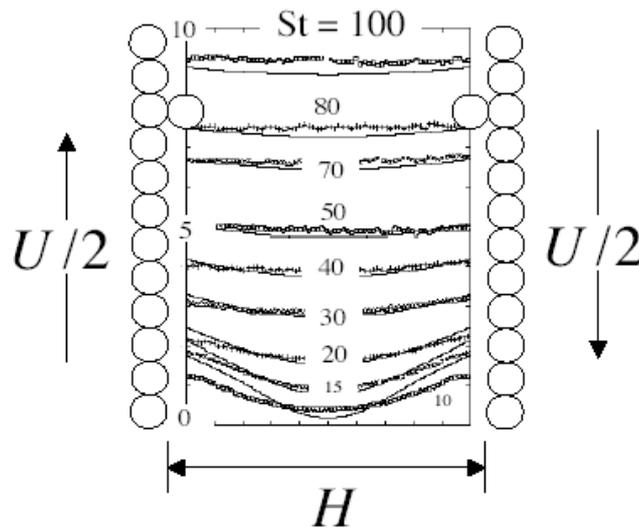

Figure 3.   Lateral profiles of dimensionless granular fluctuation velocity $[2\sqrt{T}/U][H/d]$ at values of the Stokes number shown and the conditions $H/d = 12$, $Re = 0.4$, $R_\tau = 0$ and $\bar{\nu} = 0.3$. Symbols are simulation data and lines are predictions of the theory.

Acknowledgments

References

[1] J.T. Jenkins and M.W. Richman, Grad's 13-moment system for a dense gas of inelastic spheres, *Arch. Rat. Mech. Anal.*, Vol.87, pp.355-377, 1985.

[2] J.T. Jenkins and F. Mancini, Kinetic theory for binary mixtures of smooth, nearly elastic spheres, *Phys. Fluids A*, Vol.1, pp.2050-2057, 1989.

[3] M.Y. Louge, J.T. Jenkins, H. Xu, B. Arnarson, Granular segregation in collisional shearing flows, in: A. Aref, J.W.Phillips (Eds.), *Mechanics for a New Millennium*, Kluver Academic Publishers, pp.239-252, 2001.

[4] H. Xu, M.Y. Louge, A. Reeves, Solutions of the Kinetic Theory for Bounded Collisional Granular Flows, *Continuum Mech. Thermodyn.*, Vol.15, pp.321-349, 2003.

[5] A.S. Sangani, G. Mo, H.-K. Tsao, D.L. Koch, Simple shear flows of dense gas-solid suspensions at finite Stokes number, *J. Fluid Mech.*, Vol.313, pp.309-341, 1996.

[6] H. Xu, M.Y. Louge, J.T. Jenkins, Flow development of a gas-solid suspension in a microgravity Couette apparatus, *Conference and Exhibit on International Space Station Utilization, Cape Canaveral, FL, Oct. 15-18, 2001*, AIAA-2001-4992, NY, 2001.

[7] H. Xu, Collisional Granular Flows with and without Gas Interaction in Microgravity, Cornell University, 2003.

[8] H. Xu, A. Reeves, M.Y. Louge, Measurement Errors in the Mean and Fluctuation Velocities of Spherical Grains from a Computer Analysis of Digital Images, *Rev. Sci. Instrum.*, Vol.75, pp.811-819, 2004.

[9] A.J.C. Ladd, Numerical simulations of particulate suspension via a discretized Boltzmann equation, *J. Fluid Mech.*, Vol.271, pp.285-339, 1994.

[10] H. Xu, M.Y. Louge, J.T. Jenkins, Flow development of a sheared collisional granular flow, in: Y. Kishino (Eds.), *Powders and Grains*, pp.259-262, Swets & Zeitlinger, Lisse, 2001.

[11] J.T. Jenkins, B. Arnarson, Private Communication, 2000.

[12] H. Xu, R. Verberg, D.L. Koch, M.Y. Louge, Dense bounded shear flows of agitated solid spheres in a gas at intermediate Stokes and finite Reynolds numbers, *J. Fluid Mech.*, under review, 2004.

[13] J. Happel, H. Brenner, Low Reynolds number hydrodynamics, Prentice-Hall, NY, 1965.

[14] P.C. Carman, The determination of the specific surface area of powder, *I. J. Soc. Chem. Ind.*, Vol.57, pp.225-236, 1937.

[15] M.A. van der Hoef, R. Beetstra, J.A.M. Kuipers, Lattice Boltzmann simulations of low Reynolds number flow past mono- and bidisperse arrays of spheres: results for the permeability and drag force, *J. Fluid Mech.*, under review, 2004.

[16] J.T. Jenkins, C. Zhang, Kinetic theory for identical, frictional, nearly inelastic spheres, *Phys. Fluids*, Vol.14, pp.1228-1235, 2002.

[17] I. Goldhirsch, Rapid Granular Flows, *Ann. Rev. Fluid Mech.*, Vol.35, pp.267-293, 2003.

[18] D.L. Koch, Kinetic theory for a monodisperse gas-solid suspension, *Phys. Fluids A*, Vol.2, pp.1711-1723, 1990.

[19] R.R. Sundararajakumar, D.L. Koch, Non-continuum lubrication flows between particles colliding in a gas, *J. Fluid Mech.*, Vol.313, pp.283-308, 1996.

[20] J.J. Wylie, D.L. Koch, A.J.C. Ladd, Rheology of suspensions with high particle inertia and moderate fluid inertia, *J. Fluid Mech.*, Vol.480, pp.95-118, 2003.

[21] R. Verberg, D.L. Koch, Rheology of suspensions with low to moderate fluid inertia at finite Stokes number, *J. Fluid Mech.*, in preparation, 2004.

[22] D.L. Koch, A.S. Sangani, Particle pressure and marginal stability limits for a homogeneous monodisperse gas fluidized bed: kinetic theory and numerical simulations, *J. Fluid Mech.*, Vol.400, pp.229-263, 1999.

[23] J.T. Jenkins, M.Y. Louge, On the flux of fluctuation energy in a collisional grain flow at a flat, frictional wall, *Phys. Fluids*, Vol.9, pp.2835-2840, 1997.

[24] M.A. Hopkins, M.Y. Louge, Inelastic Microstructure in Rapid Granular Flows of Smooth Disks, *Phys. Fluids A*, Vol.3, pp.47-57, 1991.